THE DESIGN AND SYNTHESIS OF NUCLEAR LOCALIZATION SIGNAL (NLS) MIMICS

A Senior Thesis

By

Thai Huu Ho

1997-98 University Undergraduate Research Fellow

Texas A&M University

Group: Biochemistry/Chemistry

The Design and Synthesis of Nuclear Localization Signal (NLS) Mimics

by

Thai Huu Ho

Submitted to the
Office of Honors Programs and Academic Scholarships
Texas A & M
University in partial fulfillment of the requirements for

1997-98 UNIVERSITY UNDERGRADUATE RESEARCH FELLOWS PROGRAM

April 16, 1998

Approved as to style and content by:

Robert F. Standaert (Faculty Advisor)
Department of Chemistry

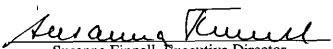

Susanna Finnell, Executive Director
Honors Programs and Academic Scholarships

Table of Contents

The Design and Synthesis of Nuclear Localization Signal (NLS) Mimics

Thai Huu Ho, (Dr. Robert F. Standaert)
University Undergraduate Fellow, 1996-1997, Texas A & M University
Department of Chemistry

Nuclear import of proteins is a carefully controlled process that is critical for cellular function and regulation. A protein is marked for nuclear entry by a nuclear localization signal (NLS), a peptide motif which typically consists of one or two small clusters rich in basic amino acids (lysine or arginine). Transport occurs through pores that span the nuclear envelope by a receptor mediated, energy-dependent process.

The goal of this study is to synthesize mimics of the NLS from aminoalkylated dihydroxybenzene fragments joined with linkers of various length, rigidity and directional constraint. The project is part of a larger effort to understand the molecular recognition in nuclear protein import; its emphasis is to study the role of charge placement, orientation, and linker features in NLS recognition. Modeled after the NLS of the HIV-1 matrix protein, the proposed molecules can mimic the side chain placement of the NLS template. Candidates are evaluated for inhibition in an *in vitro* nuclear import assay.

Inhibition was not observed for all the candidates despite the presence of positively charged clusters. The results suggest inhibition is not solely based on the presence of positive charge and confirms the hypothesis that other factors, such as orientation, are important.

Introduction

Nuclear import of proteins is a carefully controlled process that is critical for cellular function and regulation. A protein is marked for nuclear entry by a nuclear localization signal (NLS), a peptide motif which typically consists of one or two small clusters rich in basic amino acids (lysine or arginine). Transport occurs through pores that span the nuclear envelope by a receptor mediated, energy-dependent process. The goal of this study is to synthesize mimics of the NLS from aminoalkylated dihydroxybenzene (resorcinol) fragments joined with linkers of various length, hydrophobicity, H-bonding ability, rigidity and directional constraint (Figure 1). Modeled after the NLS of the HIV-1 matrix protein, the proposed molecules can mimic the side chain placement of the NLS template and will test the importance of other features for recognition. Candidates will be evaluated by an *in vitro* nuclear import assay. The project is part of a larger effort to understand the molecular recognition in nuclear protein import; its emphasis is to study the role of charge placement, orientation, and linker features in NLS recognition. The information gained will provide clues to the structure required for nuclear import and will be applied to the development of more sophisticated NLS mimics.

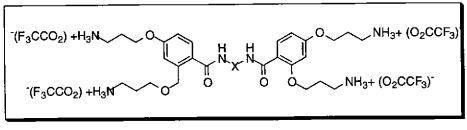

Figure 1: Proposed aminoalkylated resorcinol derivatives

Background

Cellular functions are often controlled at the molecular level. Such is the case for the macromolecular movement between the nucleus and the cytoplasm, which is an important process for both normal cells and for viruses such as HIV-1 (Bukrinsky et al., 1992). Small molecules of up to 20-40 kDa passively diffuse through the nuclear pores while larger proteins must be actively transported.

The mechanism of nuclear import (Figure 2) and the molecules involved are still being elucidated, but the process occurs in two macroscopic steps (Richardson et al., 1988):
1) The import substrate's NLS is recognized by a cytosolic receptor called importin (also called karyopherin), a heterodimer of two subunits α and β (Blobel et al., 1995); the α subunit recognizes the NLS (Görlich et al., 1995); the β subunit docks α and the substrate at the nuclear pore complex (NPC), as well as increases the affinity of the α-NLS interaction.
2) The import substrate and α are translocated through the nuclear pore. The energy required for nuclear import is supplied at least in part by the hydrolysis of GTP by Ran, a GTPase required for import (Moroianu et al., 1996).

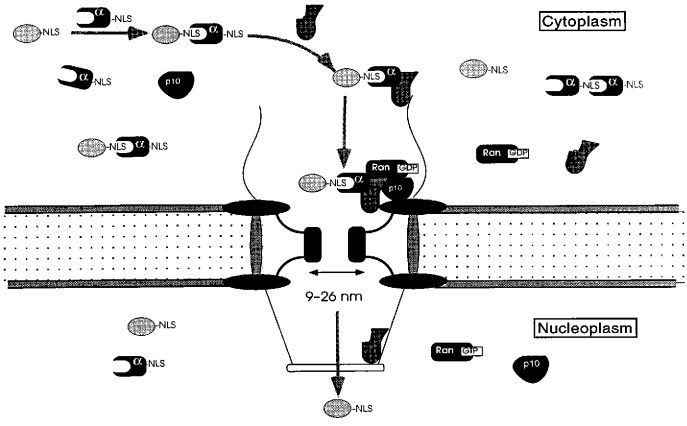

Figure 2: Model of Nuclear Import

The NLS is a peptide motif that directs the nuclear import of proteins. There is no specific consensus sequence between the known NLS peptides, but the typical sequence has a cluster of basic residues (arginine or lysine) in a 6-8 amino acid stretch (Boulikas et al., 1993). The basic residues (typically 3-5) are arranged in one or two clusters, leading to unipartite or bipartite motifs, respectively (Robbins et al., 1991).

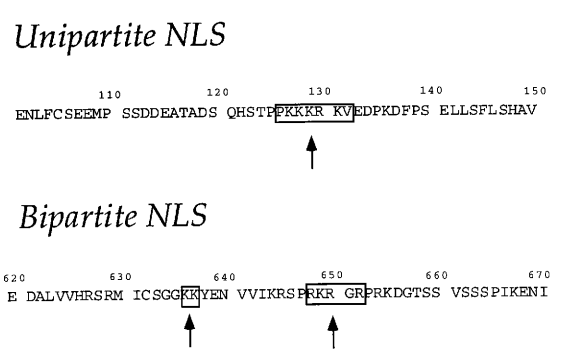

Figure 3: Examples of unipartite and bipartite NLS sequences

The prototype example of a NLS is the seven amino acid sequence PKKKRKV from the simian virus (SV40) large T-antigen (Kalderon et al., 1984). An interesting characteristic of some NLS peptides including the SV40 NLS is that they are portable (Goldfarb et al., 1986). For instance, the SV40 NLS, when attached to a non-nuclear protein, either by genetic fusion or random chemical coupling, can direct the active transport of a protein to the nucleus.

Design of NLS Mimics

The design hypothesis is that the essential feature of a functional NLS is the specific arrangement of positively charged side chains. The fact that many NLS's can function out of the context of a protein, the lack of defined secondary structure in short peptides, and the heterogeneity of known NLS peptides are all consistent with this model.

Molecular modeling based on the structure of the HIV-1 matrix protein NLS (Massiah et al., 1994) led to the identification of *meta*-disubstituted benzenes as suitable templates for the attachment of amino acid-like side chains in a way that could mimic their positions in a native NLS. The molecules are aminoalkylated resorcinol derivatives coupled with a spectrum of diamide linkers that vary in length, rigidity, and orientation. Linker variations will also explore the importance of hydrophobicity and H-bonding ability in the recognition of the NLS.

The adjacent figure is a superimposition of a template on the HIV-1 NLS. The NLS structural coordinates are gray and the sequence is shown by **1**. All of the amino acid side chains except of the lysines have been omitted. The resorcinol template is black and the aryl substituents, also the C_β's, are marked with spheres. An example of a proposed diamide linker is shown by **2**. The coordinates of the matrix protein were generously provided by Dr. Wesley Sundquist (University of Utah).

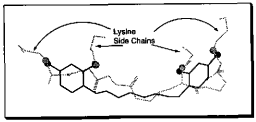

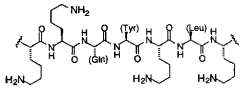

1 **KKQYKLK sequence of HIV-1 Matrix Protein NLS**

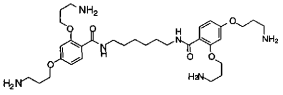

2 **Example of proposed diamide linked resorcinol template**

Figure 4: Superimposition of Template on the HIV-1 Matrix Protein NLS

Results

Synthesis of Candidates

The general synthetic strategy is to first alkylate the resorcinol fragments and then couple the fragments with a diamine linker to yield the target tetraamines. Since the alkylation step is slow, it is easier to alkylate first so that there are only mono- and di-alkyl adducts. If the alkylation was performed after the coupling, then there would be a mixture of mono-, di-, tri-, and tetra-alkyl adducts which would be harder to separate by column chromatography.

The benzoic acid **3** was converted to the corresponding methyl ester **4** using a Fischer esterification with concentrated HCl as a catalyst. A methyl ester was chosen as a protecting group because of its ease of cleavage via saponification. The protecting group also saves one equivalent of the alkylating agent because the carboxylate of **3** is a good nucleophile and can compete with the nucleophilic phenolic oxygens in the alkylation reaction.

Scheme 1

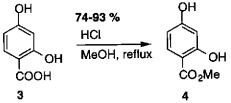

3 **4**

In the next step, the alkylating agent, 3-*tert* -butyloxycarbonyl aminopropylbromide **6**, was prepared by acylating the amino terminus of propylamine **5** with di-*tert* - butyl dicarbonate (Mulders et al., 1997). The *tert* -butyloxycarbonyl group was chosen because of its ease of cleavage with trifluoroacetic acid (TFA). The diamine linkers are acylated

by the the resorcinol fragments, so the Boc protecting group prevents undesired competing acylations of propylamine **5**.

Scheme 2

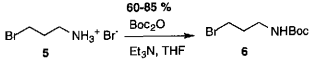

2,4-bis(3-*tert* -butoxyformamidopropyl) benzoic acid methyl ester, **7** was prepared by alkylating methyl ester **4** with **6**. Pulverized potassium carbonate served as a weak base to deprotonate the hydroxyl groups so that the phenolic oxygens could serve as nucleophiles to displace the bromine from the alkylating agent. The weak base, K_2CO_3, was used to prevent any undesired elimination of the bromine (Mulders et al., 1997). The resulting product is a mixture of mono- and di-alkyl adducts which is easily separated by column chromatography.

Scheme 3

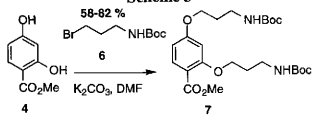

The carboxylic acid **8** was prepared via saponifcation of **7** using a 20% MeOH/H_2O mixture with 1 M NaOH as a catalyst. The small amount of methanol is required to dissolve the methyl ester. The ester protecting group is removed so that the carboxyl group can be activated for coupling with the diamine linkers.

Scheme 4

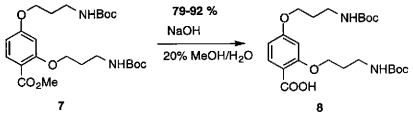

Scheme 5

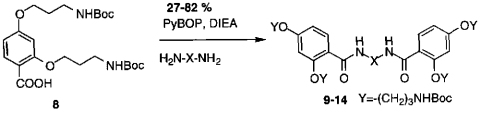

The carboxylic acid **8** was coupled to various diamine linkers (Figure 5) to afford the coupled benzamide fragments **9-14**. Each diamine linker was introduced via the peptide coupling agent PyBOP (Coste et al., 1990). PyBOP activates the carboxyl group by the formation of an active ester which then acylates the diamine to yield the diamide.

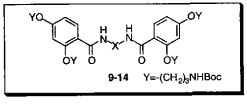

Compound	-X-
9	-$(CH_2)_2$-
10	-$(CH_2)_4$-
11	-$(CH_2)_6$-
12	-$(CH_2)_8$-
13	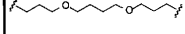
14	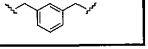

Figure 5: Linkers

Scheme 6

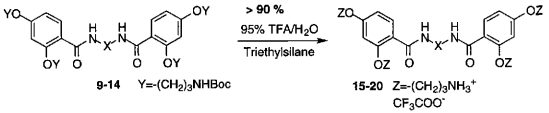

The final tetraamine TFA salts **15-20** were prepared in quantitative yields by deprotection of the Boc groups using 95% TFA/ 5% H_2O. Triethylsilane was added to scavenge any *tert* -butyl cations. The final products were prepared as TFA salts rather than the tetraamines because of the water solubility and the shelf stability of the salts.

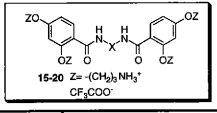

Compound	-X-
15	-$(CH_2)_2$-
16	-$(CH_2)_4$-
17	-$(CH_2)_6$-
18	-$(CH_2)_8$-
19	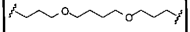
20	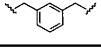

Figure 6: Tetraamine linkers

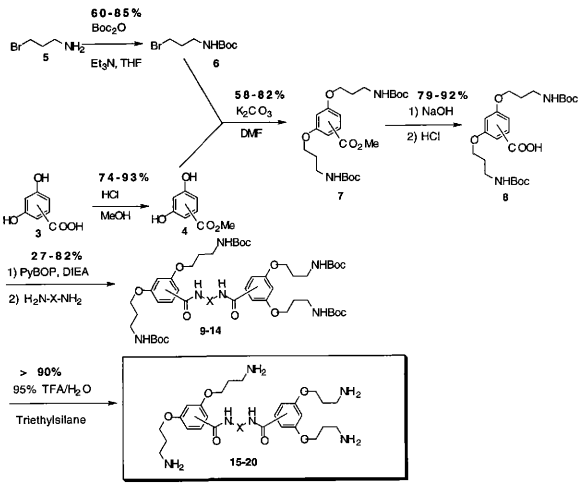

Figure 7: Overall Synthetic Scheme

Testing of Candidates

The candidates, **15-20**, were tested via the *in vitro* import assay developed by Silver and coworkers (Schlenstedt, et al., 1993). In this assay, an NLS peptide (CTPPKKKRKV) is conjugated to human serum albumin (HSA) labeled with the fluorochrome lissamine rhodamine. The protein is introduced into permeabilized *Saccharomyces cerevisiae* yeast cells and its subcellular localization is monitored by fluorescence microscopy. Since the NLS is portable, the HSA will be imported if it has been coupled to a functional NLS. In addition, nuclear import is receptor mediated and saturable, so a functional NLS mimic will competitively inhibit the nuclear uptake of the import substrate (Goldfarb et al., 1986).

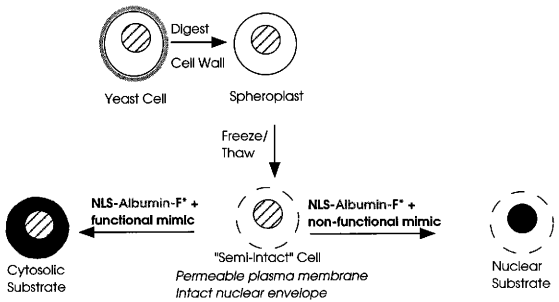

Figure 8: Nuclear Import Assay

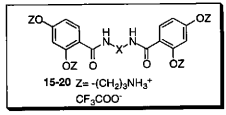

Compound	-X-	% Yield Coupling	Activity
15	-$(CH_2)_2$-	67	-
16	-$(CH_2)_4$-	82	+/-
17	-$(CH_2)_6$-	27	+
18	-$(CH_2)_8$-	58	+
19	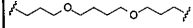	48	?
20	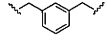	63	+/-

+/- some import observed
- import observed (no inhibition)
+ no import (inhibition)
? not tested

Figure 9: Preliminary Evaluation of Candidates

Preliminary Conclusions

Six related benzamide tetraamines (**15-20**) were synthesized to test the features important for NLS recognition (Figure 9). The molecules are aminoalkylated resorcinol derivatives coupled with a spectrum of diamide linkers that vary in length, rigidity, and orientation. Straight chain alkyl linkers ranging from two to eight carbons were chosen to explore the effects of length variations. A rigid aromatic linker and an ether linker were chosen to explore the effects of orientation, rigidity and H-bonding ability.

Although the nuclear import assay is not quantitative, it can evaluate a large library of compounds quickly and is a good initial screen for potential candidates. The candidates were classified into the following three categories depending on the extent of inhibition (Figure 9):

1) strong inhibition (+)

2) weak inhibition (+/-)

3) no inhibition (-).

The results of the preliminary evaluation can be used to direct the synthesis of more complex NLS mimics and determine the importance of functional groups in NLS recognition. Once potential candidates have been identified, more rigorous testing can be conducted to determine the nature of the inhibition.

Compounds **17** and **18** demonstrated strong inhibitory effects while **15** seemed to have no effect on nuclear import. Weak inhibition was observed for **16** and **20**. Due to time constraints, **19**, was synthesized, but has not yet been tested in the assay. Interestingly, nuclear import in the cells can be partially reconstituted in the samples (for compounds **16-18, 20**) after an additional amount of the NLS receptor, importin α, is added. There seems to be some length constraint for inhibition because the ethylene-linked dimer did not demonstrate an inhibitory effect. The weak inhibition observed for **16** and **20** suggests that linker length and flexibility may be important in NLS

recognition. The ethylene-linked dimer may be too short for the proper orientation of the propylamine side chains. Although the typical NLS sequence has a cluster of basic residues (arginine or lysine), inhibition was not observed for all the candidates despite the presence of positively charged clusters. The results of this study suggest inhibition is not solely based on the presence of positive charge and confirms the hypothesis that other factors, such as orientation, are important.

Future Studies

The compounds synthesized are relatively simple in functionality and seem to meet the minimum requirements for the inhibition of nuclear import. Compounds with different linkers such as diesters, diethers, and oligopeptides can be synthesized to further test the relevant features of NLS recognition. In addition, testing compounds with similar lengths, but different functionalities will test the hypothesis that recognition is based on charge and that backbone features are unimportant.

Although it has been shown that the benzamide tettraamines can inhibit nuclear import, it is not clear where the NLS mimics interact with the nuclear import machinery. Since the assay is not quantitative, more stringent tests should be conducted with potential candidates. In the next phase of testing, the NLS mimics should be conjugated to a non-nuclear protein. Since the NLS is portable, conjugation of the protein to a functional NLS mimic should direct the protein into the nucleus. In addition, binding constants between the NLS receptor, importin α, and the NLS mimics should be measured to demonstrate the interaction between the mimics and the receptor.

Experimental Section

Synthetic Procedures

The ^{1}H and ^{13}C NMR spectra were obtained on a Varian Unity Plus 300 (^{1}H 299.961 MHz; ^{13}C, 75.432 MHz) spectrometer and are referenced to the deuterium lock signal from the sample solvent. Analytical thin-layer chromatography (TLC) was carried out on precoated plates (silica gel 60, Merck, F_{254}), and the spots were visualized with UV light and stained with either ninhydrin, potassium permanganate, or in an iodine chamber. Column chromatography was performed with 230-400 mesh silica gel. Mass spectral data was collected by the Texas A & M Mass Spectrometry Applications Laboratory. Unless otherwise specified, all solvents and reagents were obtained from commercial suppliers and used without further purification.

Methyl 2,4 dihydroxy benzoate (4)

In a 500 mL round-bottom flask equipped with a magnetic stir bar was placed 2,4 dihydroxybenzoic acid (5.00 g, 32.44 mmol, 1 equiv). 350 mL of methanol was added to dissolve the solid acid. 40 mL of concentrated HCl was then added. After 48 hours of reflux, the reaction was cooled to room temperature and the solution was neutralized to a pH of 6.8 with concentrated NH_4OH. The solution was concentrated under reduced pressure and then taken up in 250 mL of brine. The aqueous solution was extracted with ether (3 x 100 mL). The organic layers were combined, washed with saturated $NaHCO_3$ (250 mL), anhydrous Na_2SO_4, filtered and concentrated under reduced pressure to yield methyl 2,4 dihydroxy benzoate 4.06 g (74 %) as a pink brown solid.

M.W.: 168.15

MS: (+FAB/DP) *m/z* 169 ($M+ H^+$)

TLC: R_f=0.63 (1:1 ethyl acetate:hexanes)

3-*tert* -butyloxycarbonyl aminopropylbromide (6)

In a flame dried 100 mL round bottom flask equipped with a magnetic stir bar was placed 3-bromopropylamine hydrobromide (4.16 g, 19 mmol, 1 equiv). 25 mL of dry THF was added to dissolve the hydrobromide salt. The solution was allowed to mix at room temperature for 1 hour under N_2. The solution was cooled to 0°C and dry triethylamine (5.56 mL, 39.9 mmol, 2.1 equiv) and di-*t*-butyl carbonate (4.80 mL, 20.9 mmol, 1.1 equiv) were alternately added over 45 minutes. The mixture was stirred for an additional 3 hours at room temperature. The reaction mixture was concentrated under reduced pressure and the resulting white slurry was taken up in 60 mL CH_2Cl_2 and extracted with 60 mL H_2O. The aqueous phase was extracted with CH_2Cl_2. The organic phases were combined, washed with saturated $NaHCO_3$, dried with anhydrous $MgSO_4$, filtered and concentrated under pressure to yield a clear oil (3.610 g, 80 %).

M.W.: 238.13

MS: (+FAB/DP) *m/z* 240 ($M + H^+$)

TLC: R_f=0.97 (1:1 ethyl acetate:hexanes)

2,4-bis(3-*tert* -butoxyformamidopropyl) benzoic acid methyl ester (7)

In a flame dried 50 mL round bottom flask equipped with a magnetic stir bar was placed methyl 2,4 dihydoxybenzoate (0.04968 g, 0.2955 mmol, 1 equiv), and pulverized K_2CO_3 (0.163 g, 1.182 mmol, 4 equiv). 1 mL of anhydrous DMF was added to form a slurry. The slurry was allowed to stir for 5 minutes under N_2 at room temperature and then the 3-*tert* -butyloxycarbonyl aminopropylbromide (0.2815 g, 1.182 mmol, 4 equiv) was added dropwise via syringe. The solution was allowed to stir under N_2 for 31 hours at room temperature. The solution was taken up in 30 mL of CH_2Cl_2 and extracted with (3 x 30 mL) H_2O. The aqueous phases were combined and extracted with (2 x 20 mL) CH_2Cl_2. The organic phases were combined, dried with brine (2 x 20 mL), anhydrous Na_2SO_4,

filtered and concentrated under reduced pressure. The dark brown oil was purified by silica gel column chromatography (ethyl acetate/hexanes 1/1) to yield (0.083 g, 58 %) a pale pink oil.

M.W.: 482.23

MS (+FAB/DP) *m/z* 483 ($M + H^+$), 505 ($M+ Na^+$)

TLC: R_f=0.51 (1:1 ethyl acetate:hexanes)

2,4-bis(3-*tert* -butoxyformamidopropyl) benzoic acid (8)

In a 250 mL round-bottomed flask equipped with a magnetic stir bar was placed 2,4-**2,4-**bis(3-*tert* -butoxyformamidopropyl) benzoic acid methyl ester (0.8095 g, 1.6786 mmol, 1 equiv). 2.01 mL of 1 M NaOH and 15 mL of 20% H_2O in MeOH was added to dissolve the ester oil. The resulting solution was heated to 60^0 C in a water bath for 24 hours. The methanol was removed under reduced pressure and the resulting aqueous solution was acidified to a pH of 4.5 with 1 M HCl. The aqueous solution was extracted with (3 x 10 mL) ether. The organic phases were combined, washed with anhydrous $MgSO_4$, filtered, and concentrated under reduced pressure to yield a (0.7235 g, 92 %) white solid.

M.W.: 468.25

MS (+FAB/DP) *m/z* 469 ($M + H^+$)

TLC: R_f=0.21 (1:1 ethyl acetate:hexanes)

Representative Procedure for coupling with PyBOP (11)

In a flame dried 50 mL round bottom flask equipped with a magnetic stir bar was placed 2,4-bis(3-*tert* -butoxyformamidopropyl) benzoic acid (0.500 g, 1.067 mmol, 2.1 equiv), PyBOP (0.556 g, 1.067 mmol, 2.1 equiv), and DIEA (400 µL, 2.297 mmol, 4.52 equiv) under N_2. Next, 20 mL of dry CH_2Cl_2 was added to dissolve the solid mixture. The solution was allowed to mix for five minutes and then the 1, 6 hexamethylene diamine (0.0591 g, 0.5085 mmol, 1 equiv) was added. The reaction was stopped after 24 hours by concentrating the solution under reduced pressure to an orange oil. The oil was loaded onto a silica column and eluted with ethyl acetate to yield a white solid (0.3756 g 71 %).

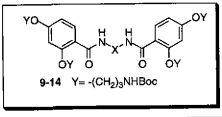

9-14 Y= -$(CH_2)_3$NHBoc

Compound	-X-	% Yield Coupling	MS (FAB)	TLC R_f (in EtOAC)
9	-$(CH_2)_2$-	67	(M+Na$^+$) 983	0.69
10	-$(CH_2)_4$-	82	(M+H$^+$) 989	0.46
11	-$(CH_2)_6$-	27	(M+Na$^+$) 1040	0.53
12	-$(CH_2)_8$-	58	(M+Na$^+$) 1068	0.64
13	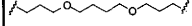	48	(M+Na$^+$) 1128	0.55
14	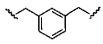	63	(M+Na$^+$) 1060	0.81

Figure 10: MS and TLC data of compounds **9-14**

Representative Procedure for Boc deprotection with 95 % TFA/ 5 %H_2O (18)

In a flame dried 50 mL round bottom flask equipped with a magnetic stir bar was simultaneously placed the diamide, **12**, (0.2692 g, 0.2576 mmol, 1 equiv) and triethylsilane (250 µL, 1.565 mmol, 6.1 equiv). 10 mL of 95% TFA/ 5 % H_2O was then added to dissolve the solid diamide. The reaction mixture was stirred at room temperature for two hours and then concentrated to a white solid under reduced pressure. The solid was taken up in 10 mL of water and extracted with (3 x 20 mL) ether. The aqueous phases were combined and then concentrated to a white solid (0.2194 g, 93 %) under reduced pressure.

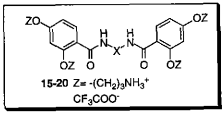

15-20 Z= $-(CH_2)_3NH_3^+$ CF_3COO^-

Compound	-X-	MS (FAB)
15	$-(CH_2)_2-$	(M+Na$^+$) 583
16	$-(CH_2)_4-$	(M+H$^+$) 589
17	$-(CH_2)_6-$	(M+Na$^+$) 639
18	$-(CH_2)_8-$	(M+H$^+$) 645
19	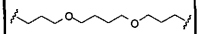	-
20	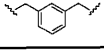	(M+Na$^+$) 659

Figure 11: MS of Compounds **15-20**

Spectral Data

(15)

M.W.: 560.31

^{1}H NMR: (CH_3OD, ppm) δ 2.01-2.14 (m, J = 6.4 Hz), 3.02-3.09 (m, J = 6.5 Hz), 4.06 (t, J = 5.9 Hz), 4.14 (t, J = 5.7 Hz), 6.50 (d, J = 2.1 Hz), 6.54 (d, J = 2.4 Hz), 6.57 (d, J = 2.1 Hz), 7.56 (d, J = 8.4 Hz).

^{13}C NMR: (CH_3OD, ppm) δ 21.90, 22.38, 32.51, 33.09, 34.59, 60.64, 62.04, 95.13, 101.46, 111.39, 126.88, 153.37, 157.85, 163.61.

(16)

M.W.: 588.40

^{1}H NMR: (CH_3OD, ppm) δ 1.56-1.60 (m, J = 3.3 Hz), 2.01-2.14 (m, J = 6.5 Hz), 3.02-3.08 (m, J = 3.7 Hz), 3.31 (t, J = 6.0 Hz) 4.06 (t, J = 5.7 Hz), 4.13 (J= 5.9 Hz), 6.52 (d, J = 2.1 Hz), 6.54 (d, J = 2.1 Hz), 6.57 (d, J = 1.8 Hz), 7.51 (d, J = 8.7 Hz).

^{13}C NMR: (CH_3OD, ppm) δ 27.84, 28.29, 38.42, 39.04, 40.39, 66.53, 67.98, 101.02, 107.25, 117.72, 132.47, 159.13, 163.57, 169.27.

(17)

M.W.: 616.35

^{1}H NMR: (CH_3OD, ppm) δ 1.34 (t, J = 7.5 Hz), 1.48-1.57 (m, J = 6.2 Hz), 2.00-2.13 (m, J = 6.5 Hz), 3.02-3.08 (m, J = 6.2 Hz), 3.25 (t, J = 7.1 Hz), 4.05 (t, J = 5.7 Hz), 4.12 (t, J = 5.9 Hz), 6.50 (d, J = 2.1 Hz), 6.53 (d, J = 2.4 Hz), 6.56 (d, J = 2.1 Hz), 7.50 (d, J = 8.4 Hz).

^{13}C NMR:(CH_3OD, ppm) δ 27.75, 27.83, 28.28, 30.47, 38.42, 39.05, 40.70, 66.53, 68.07, 101.02, 107.26, 117.75, 132.43, 159.15, 163.54, 169.22.

(18)

M.W.: 644.43

^{1}H NMR: (CH_3OD, ppm) δ 1.29 (s), 1.51 (t, J = 6.2 Hz), 2.04-2.11 (m, J = 5.6 Hz), 3.05 (t, J = 7.5 Hz), 3.24 (t, J = 6.9 Hz), 4.06 (t, J = 4.8 Hz), 4.13 (t, J = 4.5 Hz), 6.52 (s), 6.55 (s), 6.57 (s), 7.48 (d, J = 8.4 Hz).

^{13}C NMR:(CH_3OD, ppm) δ 27.80, 28.12, 28.28, 20.37, 30.53, 38.42, 39.15, 40.79, 66.51, 68.14, 101.03, 107.17, 117.92, 132.33, 159.13, 163.50, 169.29.

(19)

M.W.: 704.32

^{1}H NMR: (CH_3OD, ppm) δ 2.00–2.13 (m, J = 6.2 Hz), 3.02-3.08 (m, J = 6.1 Hz), 3.50 (s), 4.051 (t, J = 5.6 Hz), 4.13 (t, J = 5.6 Hz), 6.50 (d, J = 2.1 Hz), 6.53 (d, J = 2.3 Hz), 6.56 (d, J = 1.5 Hz), 7.56 (d, J = 8.4 Hz).

^{13}C NMR: (CH_3OD, ppm) δ 27.78, 28.26, 38.39, 38.95, 40.49, 66.53, 67.91, 101.02, 107.35, 117.25, 132.77, 159.25, 163.74, 169.48.

(20)

M.W.: 636.37

^{1}H NMR: (CH_3OD, ppm) δ 1.97-2.09 (m, J = 6.2 Hz), 2.89 (t, J = 6.5 Hz), 3.05 (t, J = 7.2 Hz), 4.03-4.08 (m, J = 4.9 Hz), 4.46 (s), 6.50 (d, J = 8.7 Hz), 7.14 (d, J = 7.8 Hz), 7.22 (d, J = 8.4 Hz), 7.58 (d, J = 8.4 Hz).

^{13}C NMR: (CH_3OD, ppm) δ 27.82, 28.26, 38.38, 38.63, 44.29, 66.53, 67.77, 100.98, 107.47, 116.98, 127.10, 127.30, 130.00, 132. 85, 140.70, 159.32, 163.78, 168.89.

Nuclear Import Assay

Yeast strains, HSA-conjugates, semi-intact cells, and cytosol were prepared as outlined in the literature by Silver (Schlenstedt, et al., 1993). The candidates were prepared by dissolving the TFA salts in 1 mL of 20 mM HEPES buffer (pH=7.0) and then diluting to the desired concentration (2 μM). Import assays were performed in buffer A (0.25 M sorbitol, 20 mM Pipes-KOH, pH=6.8, 150 mM K-acetate, 5 mM Mg-acetate, filter sterilized with a 0.2 μm filter) and contained 5 x 10^7 semi-intact cells/mL, 1 mM ATP, 0.1 mg/mL creatine kinase, 10 mM creatine phosphate, 2 mg/mL cytosolic proteins, 2.5 μM CTPPKKKRKV (conjugated to lissamine rhodamine labeled HSA), and 2 μM of the candidates. Semi-intact cells were visualized with DAPI (4', 6' diamidino-2-phenylindole) staining using a Zeiss Axiophot epifluorescence microscope. The samples were then incubated for 20 minutes at 20°C.

Import and inhibition were assessed by the ratio of cells with fluorescent nuclei (due to import of the rhodamine-labeled NLS HSA substrate) to the number of competent semi-intact cells (presence of DAPI staining of the nuclei, but no visible cell wall). The candidates were classified into three categories depending on the extent of inhibition (Reedy, B. of Standaert, R.F. lab, unpublished results). The extent of inhibition was evaluated by a reduction in the ratio of fluorescent nuclei to competent cells. Strong inhibition (+) is defined as a 90-100 % decrease in the ratio with respect to the samples without any inhibitor (almost no nuclei are fluorescent). Weak inhibition (+/-) is defined as a 30 to 90 % reduction (few nuclei are fluorescent). A reduction of less than 30 % was considered to be not significant (-). An additional 0.1 mg/mL of karyopherin/importin α was added for the compounds that demonstrated an inhibitory effect to see if nuclear import could be reconstituted.

Acknowledgments

This work was supported by grants from Pfizer Pharmaceuticals and from the University Undergraduate Research Fellows Program. I thank Brian Michael Reedy for preparing and performing the nuclear import assay and Mike Van Brunt for recording all the NMR spectra. I also thank Dr. R. F. Standaert, Michael Connolly, Zhi Lai, Seung-Bum Park, and Shawn Schiller for the technical assistance, illustrations and discussions.

References

Blobel J., Hijikata, M.,Moroianu, G. & Radu, A. (1995). Mammalian karyopherin alpha 1 beta and alpha 2 beta heterodimers: alpha 1 or alpha 2 subunit binds nuclear localization signal and beta subunit interacts with peptide repeat-containing nucleoporins. *Proc. Natl. Acad. Sci. U.S.A.* **92**, 6532-6536.

Bukrinsky, M. I., et al. (1992). Active nuclear import of human immunodeficiency virus type 1 preintegration complexes. *Proc. Natl. Acad. Sci. U.S.A.* **89**, 6580–6584.

Boulikas, T. (1993). Nuclear localization signals (NLS). *Crit. Rev. Eukar. Gene Exp.* **3**, 193–227.

Coste, J., Le-Nguyen, D. & Castro, B. (1990) PyBOP: A Peptide Coupling Reagent Devoid of Toxic By-Product. *Tetrahedron Letters* **31**, 205-208.

Goldfarb, D. S., Gariépy, J., Schoolnik, G. & Kornberg, R. D. (1986). Synthetic peptides as nuclear localization signals. *Nature* **322**, 641–644.

Görlich, D., et al. (1995). Two different subunits of importin cooperate to recognize nuclear localization signals and bind them to the nuclear envelope. *Curr. Biol.* **5**, 383-392.

Kalderon, D., Richardson, W. D., Markham, A. F. & Smith, A. E. (1984). Sequence requirements for nuclear location of simian virus 40 large-T antigen. *Nature* **311**, 33.

Massiah, M. A., et al. (1994). Three-dimensional structure of the human immunodeficiency virus type 1 matrix protein. *J. Mol. Biol.* **244**, 198-223.

Matthews, S., et al. (1994). Structural similarity between the p17 matrix protein of HIV-1 and interferon-gamma. *Nature* **370**, 666-668.

Moroianu, J., Blobel, G. & Radu, A. (1996). Nuclear protein import - Ran-GTP dissociates the karyopherin alpha-beta heterodimer by displacing alpha from an overlapping binding site on beta. *Proc. Natl. Acad. Sci. U.S.A.* **93**, 7059-7062.

Mulders, S. J. E., Brouwer, A.J., & Liskamp, R. M. J., (1997). Molecular Diversity of Novel Amino Acid Based Dendrimers. *Tetrahedron Letters* **38**, 3085-3088.

Mulders, S. J. E., Brouwer, A.J., van der Meer, P. G. J., & Liskamp, R. M. J., (1997). Synthesis of a Novel Amino Acid Based Dendrimer. *Tetrahedron Letters* **38**, 631-634.

Richardson, W. D., Mills, A. D., Dilworth, S. M., Laskey, R. A. & Dingwall, C. (1988). Nuclear protein migration involves two steps: rapid binding at the nuclear envelope followed by slower translocation through nuclear pores. *Cell* **52**, 655–664.

Robbins, J., Dilworth, S. M., Laskey, R. A. & Dingwall, C. (1991). Two interdependent basic domains in nucleoplasmin nuclear targeting sequence: identification of a class of bipartite nuclear targeting sequence. *Cell* **64**, 615–623.

Schlenstedt, G., Hurt, E., Doye, V. & Silver, P. A. (1993). Reconstitution of nuclear protein transport with semi-intact yeast cells. *J. Cell Biol.* ***123***, 785–798.

Schlenstedt, G., Hurt, E., Doye, V. & Silver, P. A. (1993). Reconstitution of nuclear protein transport with semi-intact yeast cells. *J. Cell Biol.* ***123***, 785–798.